



# Thermal decomposition behavior of poly(propylene carbonate) in poly(propylene carbonate)/poly(vinyl alcohol) blend

Shaoying Cui<sup>1</sup> · Pingfu Wei<sup>1</sup> · Li Li<sup>1</sup>

Received: 5 February 2018 / Accepted: 9 April 2018 / Published online: 23 April 2018  
© Akadémiai Kiadó, Budapest, Hungary 2018

## Abstract

To provide guidance for the practical thermal processing and applications of poly(propylene carbonate)/poly(vinyl alcohol) (PPC/PVA) blend, an environmentally friendly material with wide potential applications, thermogravimetric analysis (TG) and thermogravimetric-Fourier transform infrared spectroscopy (TG-FTIR) were adopted to investigate the thermal decomposition behavior of PPC in PPC/PVA blend for its worse high-temperature thermal stability, and the decomposition processes were analyzed by Chang's method. Accordingly, the precise kinetic parameters of each thermal decomposition process were calculated by Flynn–Wall–Ozawa method. The results showed that neat PPC underwent three pyrolysis stages: unzipping, unzipping and chain random scission and unzipping. For PPC/PVA blend, the elimination reaction of the side-hydroxyl groups of PVA promoted the chain random scission of PPC, thus playing the dominant role in the thermal decomposition of PPC. The more the hydroxyl groups in PVA were, the lower the thermal stability of the blends would be. On the basis of above, a rational decomposition mechanism of PPC accelerated by PVA was proposed: With the increase in temperature, the elimination reaction of the hydroxyl groups of PVA occurred to release H<sup>+</sup> protons; then, the H<sup>+</sup> protons attacked the PPC backbone to release CO<sub>2</sub> by chain random scission, leading to a rapid mass loss of PPC in PPC/PVA blend during 200–250 °C.

**Keywords** Poly(propylene carbonate) · Poly(vinyl alcohol) · Thermal decomposition

## Introduction

With the development of society and economy, energy crisis and environmental pollution are becoming more and more serious. Therefore, an increasing number of researchers have focused on developing environmental-friendly materials, such as poly(lactic acid) (PLA), polycaprolactone (PCL), poly- $\beta$ -hydroxybutyrate (PHB), poly(butylene succinate) (PBS), cellulose, starch [1–8]. Poly(propylene carbonate) (PPC), the alternating copolymerization product of carbon dioxide and propylene oxide, is considered to be an important polymer material to reduce the emission of greenhouse gas and has attracted increasing interests for its fully biodegradability, excellent oxygen

barrier properties and biocompatibility. However, its low glass transition temperature ( $T_g$ : 20–40 °C), which leads to its brittleness below 18 °C and poor mechanical strength and dimensional stability above 40 °C, severely limits its practical applications [9]. Therefore, it is of great necessity to improve  $T_g$  and mechanical property of PPC.

In our previous work [10], based on the supramolecular science theory, polyvinyl alcohol (PVA) with multi-hydroxyl groups has been selected to melt blend with PPC to establish a unique physical cross-linked network structure by intermacromolecular hydrogen bonding between the carbonyl groups or/and the terminal hydroxyl groups of PPC and the hydroxyl groups of PVA. This interaction guarantees the good compatibility between PPC and PVA and significantly improves  $T_g$  from 34.1 °C of neat PPC to 44.0 °C of 70PPC/30PVA and the tensile strength from 10.5 MPa to a maximum value of 39.7 MPa at room temperature (23 °C) and also endows the blend with better thermal stability in the region of 100–200 °C. However, when the temperature is higher than 200 °C, the hydrogen

✉ Li Li  
powerlily@scu.edu.cn

<sup>1</sup> State Key Laboratory of Polymer Materials Engineering,  
Polymer Research Institute of Sichuan University,  
Chengdu 610065, China

bonding between PVA and PPC is damaged, resulting in the worse high-temperature thermal stability of PPC/PVA blend. This is quite different from other existing PPC-based blends, e.g., PPC/PLA, PPC/polyhydroxybutyrate valerate (PHBV), PPC/PBS, PPC/starch, PPC/cellulose acetate butyrate (CAB), whose thermal decomposition temperature is higher than that of neat PPC [11–15] and would certainly limit the practical applications of PPC/PVA blend in some special fields.

The studies on thermal decomposition behaviors of neat PPC and neat PVA have been performed extensively. As reported, PVA shows three decomposition stages including the side-groups elimination, chain scission and aromatization reaction [16–19], while PPC obeys two pyrolysis mechanisms, i.e., unzipping reaction and main chain random scission [10, 20–22]. The decomposition of PVA is mainly influenced by its hydrolysis degree, and the major factors for the decomposition of PPC are molecular mass, water, the terminal hydroxyl group and catalysts [23, 24]. But for PPC/PVA blend, no relative reports can be referred to explain this special phenomenon. In order to dig out the reasons for the accelerated high-temperature degradation of PPC in PPC/PVA blend, all the possible factors should be considered.

As known, PVA is a multi-hydroxyl polymer with strong hydrogen bonding and poor thermal processability. To match the processing temperature of PPC, water, a best plasticizer for PVA, has been adopted in our previous work to improve the melt processability of PVA. Accordingly, in our PPC/PVA blend system, due to the high purity of PPC, the factors that influence the thermal stability of PPC possibly include water and the hydroxyl groups of PVA. Therefore, in this paper, the effects of water and the hydrolysis degree of PVA on the thermal decomposition behavior of PPC are systematically studied by TG and analyzed by the nonisothermal method of Chang's method together with the isothermal method of Flynn–Wall–Ozawa method, the thermal decomposition process is further deducted from FTIR and TG-FTIR, and the degradation mechanism of PPC promoted by PVA is consequently proposed. The studies in this paper are of great significance and would offer guidance for the practical processing and applications of PPC/PVA blend, as well as the relative academic research.

## Experimental

### Materials

PPC with a number average molecular mass ( $M_n$ ) of  $1.17 \times 10^5$  was kindly provided by Changchun Institute of Applied Chemistry, Chinese Academy of Sciences. PVA-

205 with the polymerization degree of 500 and hydrolysis of 88% and PVA-105 with polymerization degree of 500 and hydrolysis degree of 99% were purchased from Kuraray Co., Japan. PVAc with polymerization degree of 630 was self-synthesized. PPC and PVA were dried in a vacuum oven at 50 °C for 24 h to, respectively, remove the residual solvent and water before processing.

### Sample preparation

PVA-205 was first plasticized by 15 mass% water to obtain the melting point of about 170 °C, which matches with the processing temperature of PPC. The plasticized PVA was then mixed with PPC in a high-speed mixer. After being fully mixed, the mixture was extruded in a single-screw extruder (RM-200C, Harbin Harpro electrical technology Co., Ltd., China) at 170 °C to obtain PPC/PVA blend. The mass ratio of PPC/PVA205 was 70:30.

To compare the effect of water and the hydrolysis degree of PVA on the thermal degradation of PPC, PPC/W with 5 mass% water, which was equal to the theoretical content of water in PPC/PVA205, PPC/PVA105 (70/30) and PPC/PVAc (70/30) were extruded in a single extruder (RM-200C, Harbin Harpro electrical technology Co., Ltd., China) at 170 °C. Neat PPC was also extruded at the same condition. Before being blended, PVA105 was plasticized with 25 mass% water to match the processing temperature of PPC.

### Characterization

Thermogravimetric analysis (TG) measurements were examined on a Q50 instrument (TA Instrument Co., Ltd., USA) under a nitrogen protective atmosphere from room temperature to 600 °C at heating rates of 2, 5, 10 and 20 °C min<sup>-1</sup>.

Thermogravimetric-Fourier transform infrared spectroscopy (TG-FTIR) was performed using a SDT Q600 V20.5 Build 15 instrument that was interfaced to a Nicolet IS10 FTIR spectrometer (Thermo Scientific Co., Ltd., USA). About 5.0 mg sample was put in an alumina crucible and heated from 50 °C to 600 °C in nitrogen atmosphere. The heating rate was 10 °C min<sup>-1</sup>, and the flow rate of nitrogen atmosphere was 60 mL min<sup>-1</sup>. FTIR spectra were obtained from 4000 to 400 at 4 cm<sup>-1</sup> resolution and 8 scans s<sup>-1</sup>.

Prior to all the tests, the samples were dried under air blasting at 80 °C for 2 days to remove the residue water except for PPC/W.

## Theoretical analysis

The basic equation of the thermal decomposition of a polymer could be expressed as follows:

$$\frac{d\alpha}{dt} = A \exp\left(-\frac{E}{RT}\right) f(\alpha) \quad (1)$$

where  $\alpha$ ,  $t$ ,  $A$ ,  $E$ ,  $R$  are the degree of decomposition (mass of polymer volatilized/initial mass of polymer), the time, the pre-exponential factor, the activation energy and the universal gas constant, respectively.

## Nonisothermal method

Chang's method [25], proposed by Wally L. Chang in 1994, was one of the nonisothermal methods to analyze the thermal decomposition kinetics of the TG curves tested at a constant heating rate. From the linear parts obtained by nonisothermal method, different thermal decomposition processes could be identified easily. According to Chang's method, if the reaction of polymer degradation is assumed to be a simple  $n$ th-order reaction,  $f(\alpha)$  could be written as follows:

$$f(\alpha) = (1 - \alpha)^n \quad (2)$$

Then, a new equation could be obtained by combining Eqs. (1) and (2).

$$\frac{d\alpha}{dt} = A(1 - \alpha)^n \exp\left(-\frac{E}{RT}\right) \quad (3)$$

Equation (3) could be further rewritten as

$$\ln\left(\frac{d\alpha}{dt}\right) - n \ln(1 - \alpha) = \ln A - \frac{E}{RT} \quad (4)$$

The plot of the left part in Eq. (4) versus  $1/T$  is a straight line when the selected  $n$  value is correct.

To investigate the thermal decomposition of PPC in PPC/PVA blend above 200 °C, Chang's method was adopted to calculate the kinetic parameters, and several values of  $n$  were assumed, i.e., 1.0, 1.5, 2.0, 2.5, 3.0. The results showed that when  $n$  was 2.5, the good linear relationships were obtained at the linear parts.

## Isothermal method

Compared with nonisothermal method, isothermal method that uses multiple heating rate programs is recommended for the calculation of the reliable kinetic parameters [26]. In this study, the integral method, Flynn–Wall–Ozawa (F–W–O) method [27–30], was utilized to calculate the activation energy of each thermal decomposition process obtained by Chang's method. The major advantage of this method is that it does not require any assumptions

concerning the form of the kinetic equation other than the Arrhenius-type temperature dependence. Equation (1) was integrated, and Doyle approximation [31] was applied to obtain Eq. (1).

$$\lg \beta = -0.4567 \frac{E}{RT} + \lg\left(\frac{AE}{g(\alpha)R}\right) - 2.315 \quad (5)$$

When certain  $\alpha$  is chosen,  $g(\alpha)$ , the integral form of  $f(\alpha)$ , is the same at different  $\beta$ . Thus, for  $\alpha = \text{constant}$ , a plot of  $\ln \beta$  versus  $1/T$  obtained from thermal curves at several heating rates should be a straight line whose slope allows the evaluation of the activation energy  $E$ . The variations in  $E$  are related to the different mechanism and factors that influence the degradation behavior, so it is used to distinguish the different stages of the thermal degradation.

## Results and discussion

### Thermal stability

As reported [24], the plausible degradation pathways for PPC included the unzipping process, chain random scission and the attack of the terminal hydroxyl group or water onto a carbonate linkage of polymer backbone. In order to find out who, water or hydroxyl group of PVA, played the main role in the thermal stability of PPC in the blend above the temperature of 200 °C, water and PVA with different hydrolysis degrees, i.e., 99% (PVA105), 88% (PVA205) and 0% (PVAc), were selected to blend with PPC, and their TG curves are shown in Fig. 1. The corresponding thermal degradation temperatures are listed in Table 1.

Compared with neat PPC,  $T_i$  and  $T_{\max}$  of PPC/W remained unchanged, and after the complete evaporation of

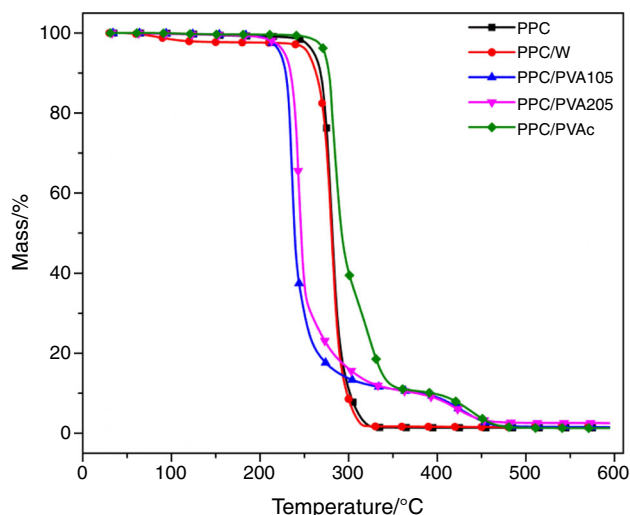


Fig. 1 TG curves of PPC, PPC/W, PPC/PVA105, PPC/PVA205 and PPC/PVAc blends at a heating rate of 10 °C min<sup>-1</sup>

**Table 1** Thermal degradation temperature of PPC and PPC blends

Sample	PPC	PPC/W	PPC/PVA105	PPC/PVA205	PPC/PVAc
$T_i/^\circ\text{C}$	269.6	269.2	229.7	236.4	276.4
$T_{\max}/^\circ\text{C}$	281.0	281.1	235.6	244.6	283.3

$T_i$ , initial degradation temperature by extrapolation method;  $T_{\max}$ , temperature of maximum loss rate

water, PPC/W presented the same TG curve as PPC, implying that water almost had no effect on the thermal decomposition of PPC. With the incorporation of PVA into PPC, the thermal degradation of the blend significantly took place ahead, and both  $T_i$  and  $T_{\max}$  decreased, indicating that PVA had a great effect on the thermal stability of PPC in the blend system. As mentioned in our previous study [10], PVA formed hydrogen bonding with the carbonyl groups or/and the terminal hydroxyl groups of PPC, thus limiting the activity of the unzipping decomposition of PPC and improving its thermal stability during 100–200 °C. However, with the increase in the temperature, the hydrogen bonding between PVA and PPC was gradually damaged, making more hydroxyl groups in PVA recovered to be eliminated or attack PPC, resulting in the decrease in the thermal stability of PPC/PVA blend, which reflected in TG curve of PPC/PVA by the rapid mass loss during the temperature range of 200–250 °C. Compared the TG curves of PPC/PVA205 with that of PPC/PVA105, it could be concluded that PVA105 with more hydroxyl groups played greater role in the thermal stability of the blend and decreased  $T_i$  and  $T_{\max}$  of the blend to a larger extent, i.e., the more the hydroxyl groups in PVA were, the lower the thermal stability of PPC/PVA blends would be. The slight improvement in the thermal stability of PPC/PVAc blend above 275 °C also confirmed this conclusion.

To investigate the decomposition mechanism of PPC, PPC/W, PVA205 and PPC/PVA205 blend, their TG curves at the heating rates of 2, 5, 10 and 20 °C min<sup>-1</sup> were studied, as shown in Fig. 2. Apparently, with the increase in heating rate, each sample behaved the same changing tendency but shifted to higher temperature. As an example, the temperatures at the maximum loss rate of neat PPC were 249.3, 264.4, 281.0 and 298.6 °C, respectively, corresponding to the different heating rates. This phenomenon was resulted from the temperature retardancy.

### Kinetics of thermal decomposition

Using Chang's method, the plots of  $\ln(d\alpha/dt) - 2.5 * \ln(1 - \alpha)$  versus  $1/T$  for PPC and PPC/W were obtained, as shown in Fig. 3. It could be seen from Fig. 3 that the degradation of PPC from 240 to 320 °C presented three different linear regions, corresponding to the different degradation process.

The activation energy for PPC and PPC/W of each region was calculated by F–W–O method, the F–W–O plots are shown in Fig. 4, and calculated activation energies are shown in Table 2. Regions I and III in each curve showed almost the same activation energy, implying the same mechanism in these two regions. This thermal decomposition behavior of neat PPC was a little different from other earlier results in the literature [20–24], whose thermal decomposition stage was divided into two regions: unzipping reaction and chain random scission or chain random scission followed by unzipping reaction. Interestingly, neat PPC and PPC/W showed approximately the same Chang's curves and E values in each region, further identifying that water had minor influence on the thermal degradation of PPC.

The plots of  $\ln(d\alpha/dt) - 2.5 * \ln(1 - \alpha)$  versus  $1/T$  for PPC, PVA and PPC/PVA205 blend are shown in Fig. 5. Apparently, the curve of PPC/PVA205 blend was quite different from that of PPC, but more similar to that of PVA, further verifying the important effect of PVA on the thermal decomposition of the blend. Both the plots of PVA and PPC/PVA205 blend could be divided into three big parts, and the first part of PPC/PVA blend contained two regions. From each part and region, simple linear curves could be observed. Part 1, in the range of 200–250 °C, was corresponding to a huge mass loss of PPC/PVA205 blend (Fig. 1) mainly caused by the degradation of PPC phase because the residue mass at 250 °C was almost the same as the theoretical mass ratio of PVA in PPC/PVA205 blend, i.e., the thermal decomposition of PPC phase was occurred in advance in the presence of PVA, while neat PVA205 only had a slight mass loss in this part due to the elimination reaction of some side groups (–OH, –OCOCH<sub>3</sub>) [10] \_ENREF\_31. Part 2, in the temperature range of 250–370 °C, was approximately corresponding to the degradation step of neat PVA by combining the analyses of the TG curves of PPC and PVA. Therefore, the main reaction in Part 2 could be inferred to be the elimination reaction of the residual side groups and the chain scission of PVA. In Part 3 (370–450 °C), PPC/PVA205 exhibited the same curve slope as PVA205, indicating the same decomposition mechanism of PPC/PVA205 and PVA205, possibly due to the completely decomposition of PPC before 370 °C.

Figure 6 shows the F–W–O plots for each region of PPC/PVA205 blend and PVA205, and every calculated

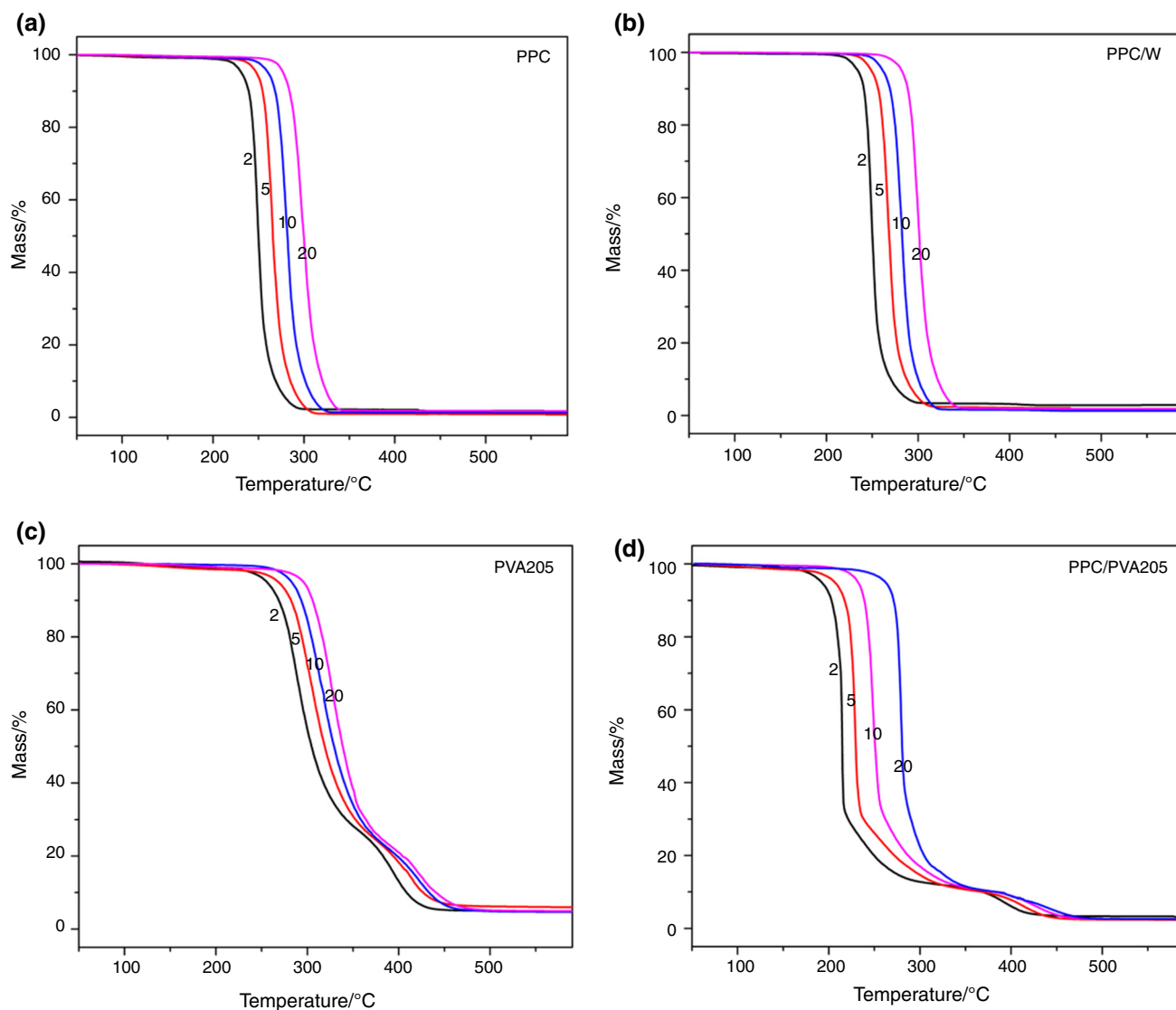


**Fig. 2** TG curves of **a** PPC, **b** PPC/W, **c** PVA205 and **d** PPC/PVA205 blend obtained at different heating rates (2, 5, 10 and 20 °C min<sup>-1</sup>)

activation energy is shown in Table 3. When PVA205 was introduced into PPC, the  $E$  values of PPC/PVA205 blend in Part 1 and Part 2 decreased significantly compared with neat PPC, leading to the accelerated thermal decomposition of PPC in the blend. It was worth noting that the  $E$  value of the blend in Part 3 (370–450 °C) remained almost unchanged compared with neat PVA, confirming that the degradation of PVA in this part had no effect on the degradation of PPC, as PPC had fully thermal decomposed before 370 °C, i.e., Part 3 mainly corresponded to the aromatization reaction of neat PVA.

### TG-FTIR analysis

TG-FTIR is a useful method to study the thermal decomposition behavior of polymers due to its direct analysis of

gas composition. Figures 7 and 8 show the 2D and 3D FTIR spectra of pyrolysates of PPC and PPC/PVA blend, respectively. For neat PPC, vibration peaks of propylene glycol ( $\nu_{\text{O-H}}$  at 3704–3125 cm<sup>-1</sup>,  $\nu_{\text{C-O}}$  at 1333–909 cm<sup>-1</sup>,  $\nu_{\text{C-H}}$  at 2971–2875 cm<sup>-1</sup>) appeared at the temperature of 188 °C, corresponding to the hydrolysates of unzipping reaction. When temperature increased to above 242 °C, a large quantity of evolved gas was produced accompanied by the start of the chain random scission of PPC, thus rendering a big mass loss in TG curve. The appearance of the characteristic vibration peaks of CO<sub>2</sub> ( $\nu_{\text{C=O}}$  at 2358 and 2314 cm<sup>-1</sup>) and cyclic propylene carbonate ( $\nu_{\text{C=O}}$  at 1860 cm<sup>-1</sup>,  $\nu_{\text{C-H}}$  at 2986–2937 cm<sup>-1</sup>,  $\nu_{\text{C-O-C}}$  at 1183–1052 cm<sup>-1</sup>) at the temperature of 242 °C demonstrated the occurrence of the chain random scission and unzipping reaction, respectively. As the further rising of

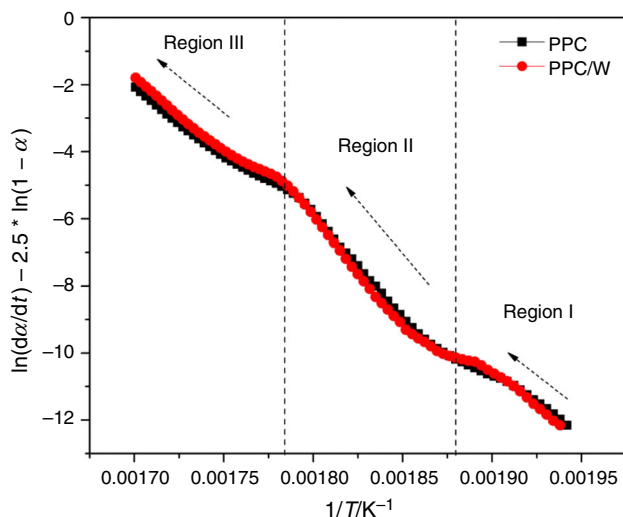


**Fig. 3** Plots of  $\ln(d\alpha/dt) - 2.5 * \ln(1 - \alpha)$  versus  $1/T$  for PPC and PPC/W by Chang's method at a heating rate of  $10 \text{ }^\circ\text{C min}^{-1}$

temperature, the intensity of  $\text{CO}_2$  peak increased first and then decreased, lastly disappeared at  $325 \text{ }^\circ\text{C}$  (Fig. 7c, d). The intensity of C=O vibration peak also increased with the temperature and still existed at  $412 \text{ }^\circ\text{C}$ . According to the data above and the existing literature [20–24], the different thermal decomposition process of PPC could be provided as unzipping, unzipping and random chain scission and followed by unzipping again, i.e., the unzipping reaction occurred along the whole thermal decomposition process, and the random chain scission took place in the mid of the

**Table 2** Calculated activation energies of PPC and PPC/W by F–W–O method

	$E_{\text{I}}$	$E_{\text{II}}$	$E_{\text{III}}$
Neat PPC/ $\text{kJ mol}^{-1}$	104.7	112.1	105.1
PPC/W/ $\text{kJ mol}^{-1}$	105.0	109.6	105.4

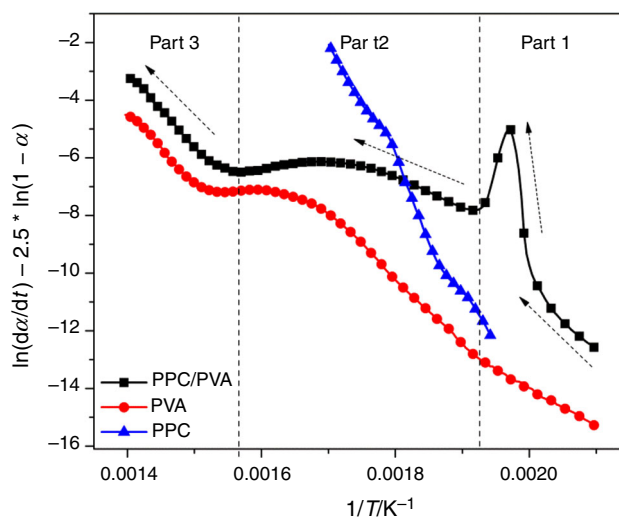


**Fig. 5** Plots of  $\ln(d\alpha/dt) - 2.5 * \ln(1 - \alpha)$  versus  $1/T$  for PPC, PVA and PPC/PVA205 blend by Chang's method at a heating rate of  $10 \text{ }^\circ\text{C min}^{-1}$

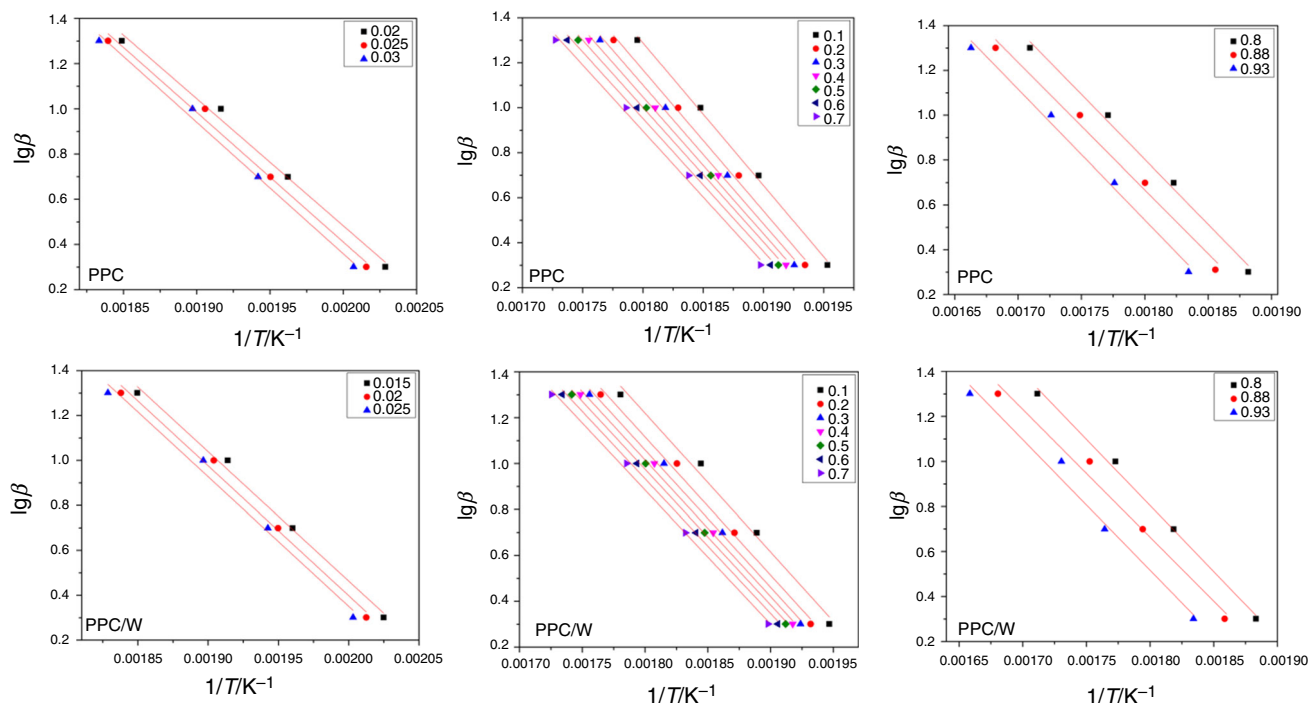


**Fig. 4** Plots of  $\lg\beta$  versus the  $1/T$  for calculating the activation energies of each region by F–W–O method of PPC and PPC/W

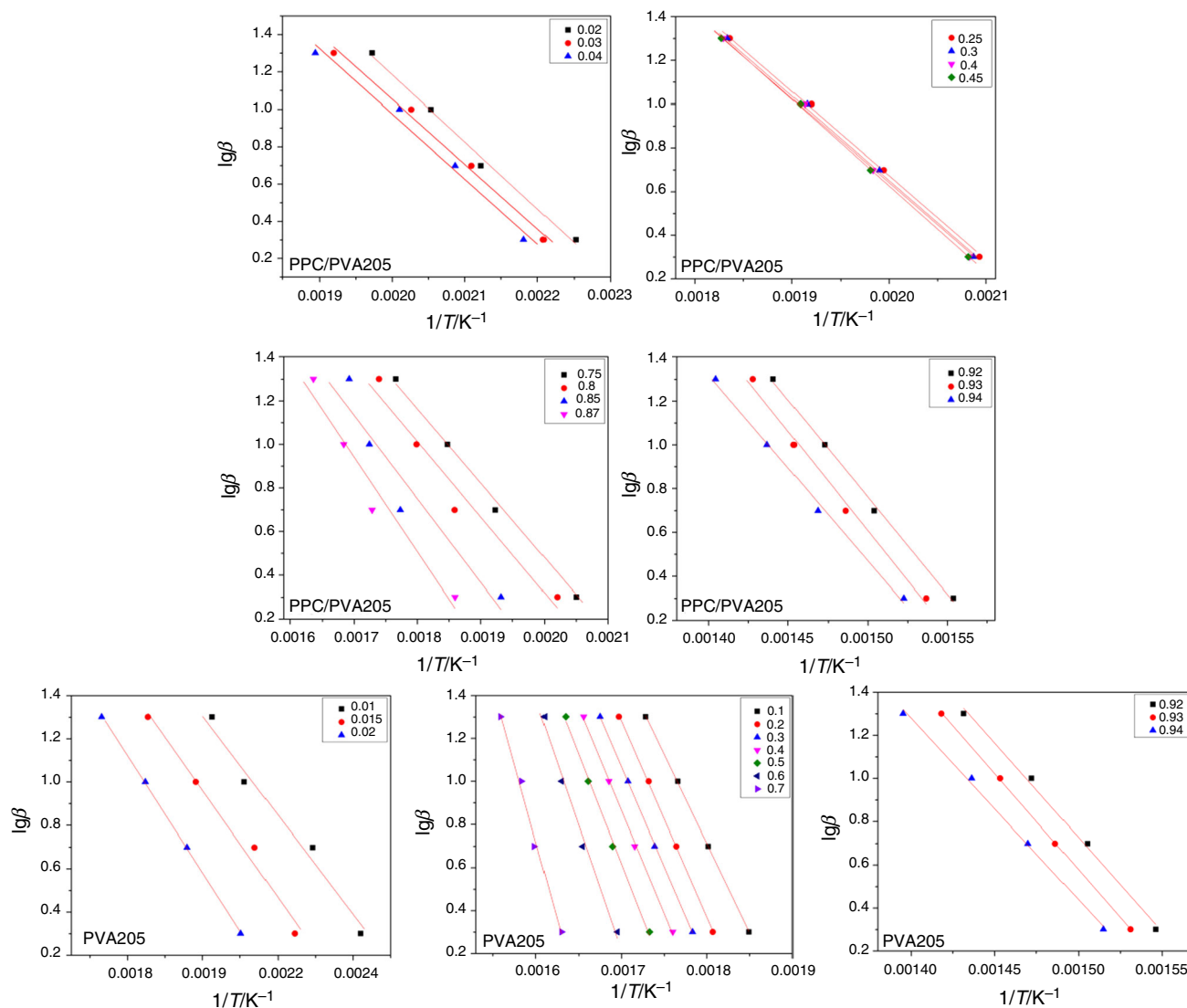


**Fig. 6** Plots of  $\lg\beta$  versus the  $1/T$  for calculating the activation energies of each region of PPC/PVA205 blend and PVA205

**Table 3** Calculated activation energies of PPC/PVA205 blend and PVA205 by F–W–O method

Sample	$E/\text{kJ mol}^{-1}$		
	Part 1	Part 2	Part 3
PPC/PVA205	58.3	69.7	160.2
PVA	39.1	175.9	157.9

decomposition process. This result was in accordance with the three regions showed in “Kinetics of thermal decomposition” section.

With the incorporation of PVA (Fig. 8), the vibration peaks of the elimination products of PVA [32, 33], i.e., C=O in acetic acid and water, were also detected at 188 °C,

accompanied by the appearance of the vibration peak of propylene glycol, the product of unzipping reaction of PPC. The peak of C=O in acetic acid and propylene glycol was still detected at 251 °C; meanwhile, the vibration peak of CO<sub>2</sub> caused by the chain random scission of PPC appeared at 203 °C and reached the highest intensity at 233 °C and then nearly disappeared at 251 °C (Fig. 5c). Obviously, the chain random scission of PPC took place in advance under the acceleration of the elimination of PVA hydroxyl groups.

Accordingly, the most possible and rational mechanism of the thermal decomposition of PPC in PPC/PVA blend could be explained as follows (Scheme 1): During the elimination process of the hydroxyl groups of PVA,  $\beta$ -H of PVA was first eliminated to generate H<sup>+</sup>; then, H<sup>+</sup> attacked the double-ester groups of PPC and accelerated the chain random scission to produce CO<sub>2</sub>; after that, H of PPC and

**Fig. 7** 3D and 2D FTIR spectra of pyrolysates from PPC

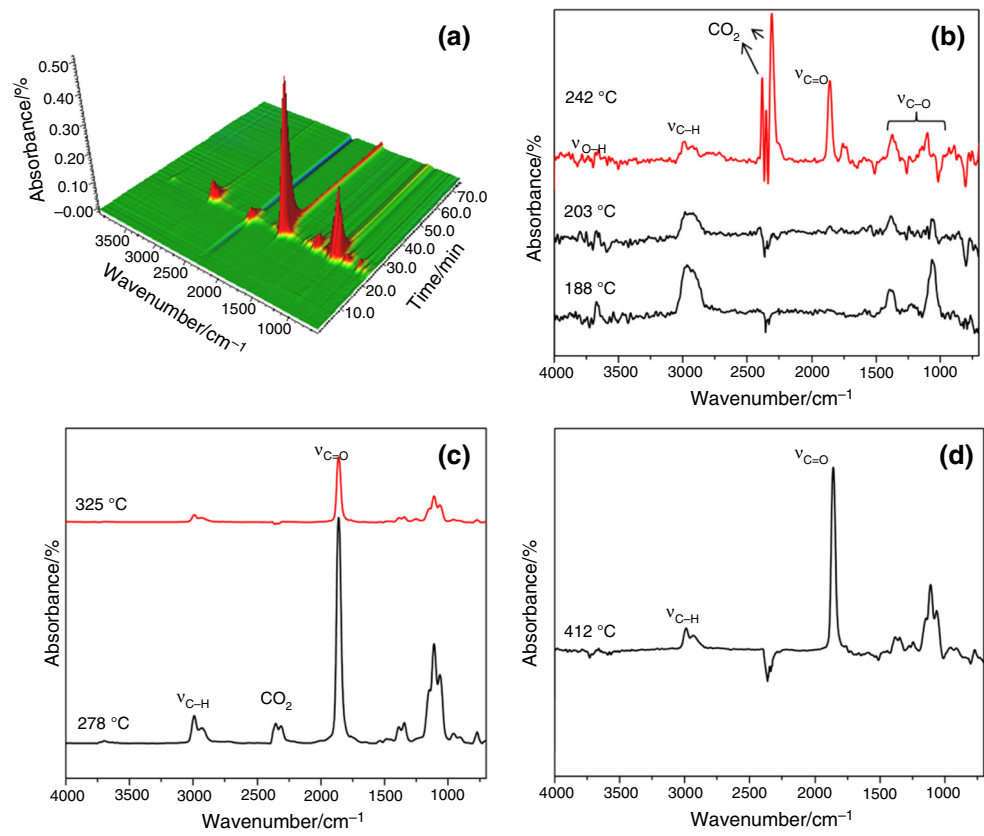
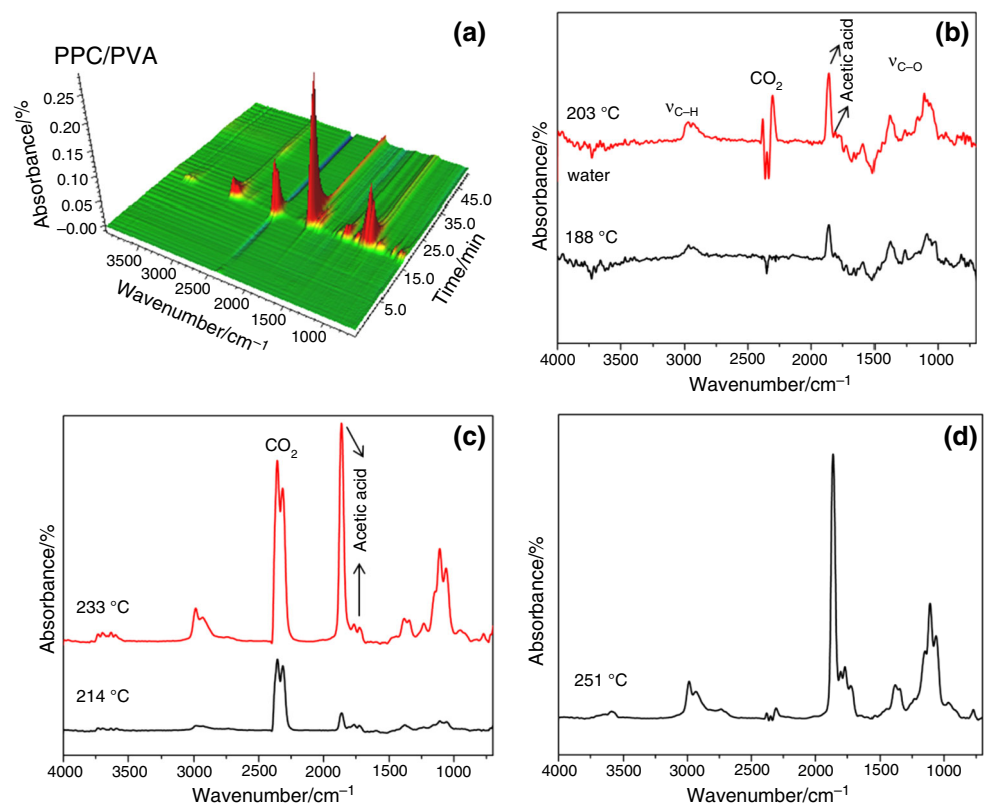
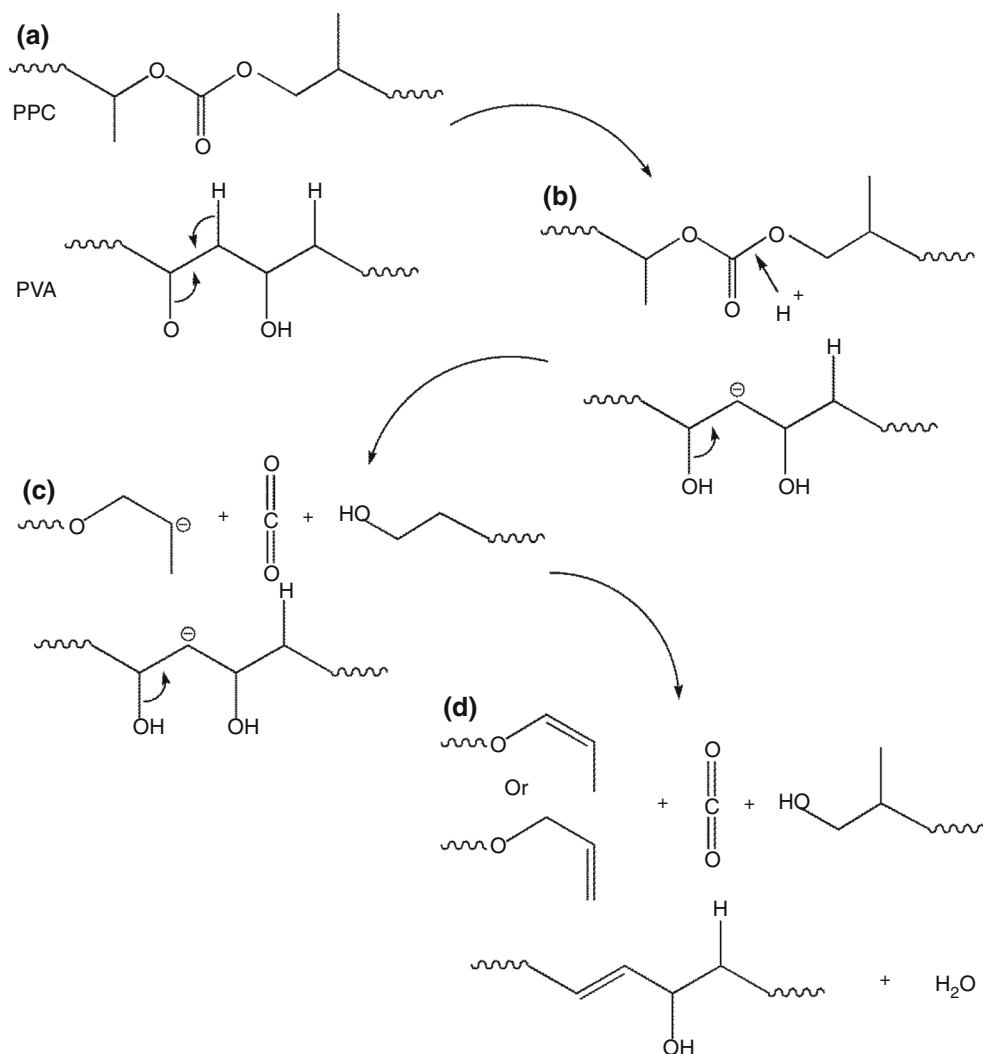


**Fig. 8** 3D and 2D FTIR spectra of pyrolysates from PPC/PVA205 blends





**Scheme 1** The mechanism of the PPC thermal decomposition promoted by PVA



the hydroxyl groups of PVA eliminated to produce water. The entire process took place instantaneously, leading to the rapid mass loss of PPC in PPC/PVA blends during the temperature from 200 to 250 °C.

## Conclusions

The effects of water and the hydroxyl groups of PVA on the thermal degradation behaviors of PPC in PPC/PVA blend were studied, the thermal decomposition processes were analyzed by Chang's method, and the degradation activation energy of each process was calculated via Flynn–Wall–Ozawa method. The results showed that neat PPC underwent three-step pyrolysis stages, i.e., unzipping reaction, unzipping reaction and chain random scission and unzipping reaction. PVA was the main reason that decreased the thermal stability of the blend ascribing to the

concurrency of the elimination reaction of the hydroxyl groups of PVA and its effect on the random scission of PPC. The more the hydroxyl content of PVA contained, the lower the thermal stability of PPC/PVA blends at the temperature above 200 °C would be. The influence of PVA on the thermal decomposition of PPC in the blend could be described as follows: The elimination of the hydroxyl groups first released  $H^+$ ; the  $H^+$  then attacked the PPC backbone to release  $CO_2$ , thus accelerating the thermal decomposition of PPC in the blend and leading to the rapid mass loss of PPC during 200–250 °C.

**Acknowledgements** This work was financially supported by the National Natural Science Foundation of China (51433006), Program of Innovative Research Team for Young Scientists of Sichuan Province (2016TD0010), Program of Introducing Talents of Discipline to Universities and State Key Laboratory of Polymer Materials Engineering (Grant No. sklpm2014-1-04).

## References

- Xing P, Ai X, Dong L, Feng Z. Miscibility and crystallization of poly( $\beta$ -hydroxybutyrate)/poly(vinyl acetate-co-vinyl alcohol) blends. *Macromolecules*. 1998;31(20):6898–907.
- Mohanty A, Misra M, Hinrichsen G. Biofibers, biodegradable polymers and biocomposites: an overview. *Macromol Mater Eng*. 2000;276(1):1–24.
- Martin O, Averous L. Poly(lactic acid): plasticization and properties of biodegradable multiphase systems. *Polymer*. 2001;42(14):6209–19.
- Vilaseca F, Mendez J, Pelach A, Llop M, Canigueral N, Girones J, et al. Composite materials derived from biodegradable starch polymer and jute strands. *Process Biochem*. 2007;42(3):329–34.
- Lim L-T, Auras R, Rubino M. Processing technologies for poly(lactic acid). *Prog Polym Sci*. 2008;33(8):820–52.
- Siró I, Plackett D. Microfibrillated cellulose and new nanocomposite materials: a review. *Cellulose*. 2010;17(3):459–94.
- Woodruff MA, Hutmacher DW. The return of a forgotten polymer—polycaprolactone in the twenty-first century. *Prog Polym Sci*. 2010;35(10):1217–56.
- Xu J, Guo BH. Poly(butylene succinate) and its copolymers: research, development and industrialization. *Biotechnol J*. 2010;5(11):1149–63.
- Luinstra GA. Poly(propylene carbonate), old copolymers of propylene oxide and carbon dioxide with new interests: catalysis and material properties. *Polym Rev*. 2008;48(1):192–219.
- Cui S, Li L, Wang Q. Enhancing glass transition temperature and mechanical properties of poly(propylene carbonate) by intermolecular complexation with poly(vinyl alcohol). *Compos Sci Technol*. 2016;127:177–84.
- Ma X, Yu J, Wang N. Compatibility characterization of poly(lactic acid)/poly(propylene carbonate) blends. *J Polym Sci Part B Polym Phys*. 2006;44(1):94–101.
- Ma X, Chang PR, Yu J, Wang N. Preparation and properties of biodegradable poly(propylene carbonate)/thermoplastic dried starch composites. *Carbohydr Polym*. 2008;71(2):229–34.
- Pang M, Qiao J, Jiao J, Wang S, Xiao M, Meng Y. Miscibility and properties of completely biodegradable blends of poly(propylene carbonate) and poly(butylene succinate). *J Appl Polym Sci*. 2008;107(5):2854–60.
- Tao J, Song C, Cao M, Hu D, Liu L, Liu N, et al. Thermal properties and degradability of poly(propylene carbonate)/poly( $\beta$ -hydroxybutyrate-co- $\beta$ -hydroxyvalerate)(PPC/PHBV) blends. *Polym Degrad Stab*. 2009;94(4):575–83.
- Xing C, Wang H, Hu Q, Xu F, Cao X, You J, et al. Mechanical and thermal properties of eco-friendly poly(propylene carbonate)/cellulose acetate butyrate blends. *Carbohydr Polym*. 2013;92(2):1921–7.
- Thomas P, Guerbois J-P, Russell G, Briscoe B. FTIR study of the thermal degradation of poly(vinyl alcohol). *J Therm Anal Calorim*. 2001;64(2):501–8.
- Dong W, Wang Y, Huang C, Xiang S, Ma P, Ni Z, et al. Enhanced thermal stability of poly(vinyl alcohol) in presence of melanin. *J Therm Anal Calorim*. 2014;115(2):1661–8.
- Taghizadeh MT, Yeganeh N, Rezaei M. The investigation of thermal decomposition pathway and products of poly(vinyl alcohol) by TG-FTIR. *J Appl Polym Sci*. 2015;132(25):42117–29.
- Wang Y, Xiang C, Li T, Ma P, Bai H, Xie Y, et al. Enhanced thermal stability and UV-shielding properties of poly(vinyl alcohol) based on Esculetin. *J Phys Chem B*. 2017;121(5):1148–57.
- Liu B, Chen L, Zhang M, Yu A. Degradation and stabilization of poly(propylene carbonate). *Macromol Rapid Commun*. 2002;23(15):881–4.
- Li XH, Meng YZ, Zhu Q, Tjong SC. Thermal decomposition characteristics of poly(propylene carbonate) using TG/IR and Py-GC/MS techniques. *Polym Degrad Stab*. 2003;81(1):157–65.
- Liu B, Zhao X, Wang X, Wang F. Thermal degradation kinetics of poly(propylene carbonate) obtained from the copolymerization of carbon dioxide and propylene oxide. *J Appl Polym Sci*. 2003;90(4):947–53.
- Peng S, An Y, Chen C, Fei B, Zhuang Y, Dong L. Thermal degradation kinetics of uncapped and end-capped poly(propylene carbonate). *Polym Degrad Stab*. 2003;80(1):141–7.
- Varghese JK, Na SJ, Park JH, Woo D, Yang I, Lee BY. Thermal and weathering degradation of poly(propylene carbonate). *Polym Degrad Stab*. 2010;95(6):1039–44.
- Chang WL. Decomposition behavior of polyurethanes via mathematical simulation. *J Appl Polym Sci*. 1994;53(13):1759–69.
- Thanki JD, Parsania PH. Dynamic DSC curing kinetics and thermogravimetric study of epoxy resin of 9,9'-bis(4-hydroxyphenyl) anthrone-10. *J Therm Anal Calorim*. 2017;130(3):2145–56.
- Ozawa T. A new method of analyzing thermogravimetric data. *Bull Chem Soc Jpn*. 1965;38(11):1881–6.
- Flynn JH, Wall LA. General treatment of the thermogravimetry of polymers. *J Res Natl Bur Stand*. 1966;70(6):487–523.
- Ozawa T. Thermal analysis—review and prospect. *Thermochim Acta*. 2000;355(1–2):35–42.
- Zanatta ER, Reinehr TO, Awadallak JA, Kleinübing SJ, dos Santos JBO, Bariccatti RA, et al. Kinetic studies of thermal decomposition of sugarcane bagasse and cassava bagasse. *J Therm Anal Calorim*. 2016;125(1):437–45.
- Doyle C. Estimating isothermal life from thermogravimetric data. *J Appl Polym Sci*. 1962;6(24):639–42.
- Ramesan MT, George A, Jayakrishnan P, Kalaprasad G. Role of pumice particles in the thermal, electrical and mechanical properties of poly(vinyl alcohol)/poly(vinyl pyrrolidone) composites. *J Therm Anal Calorim*. 2016;126(2):511–9.
- Taghizadeh MT, Yeganeh N, Rezaei M. Kinetic analysis of the complex process of poly(vinyl alcohol) pyrolysis using a new coupled peak deconvolution method. *J Therm Anal Calorim*. 2014;118(3):1733–46.